

## KINEMATICS OF FLAP-BOUNDING FLIGHT IN THE ZEBRA FINCH OVER A WIDE RANGE OF SPEEDS

BRET W. TOBALSKE\*, WENDY L. PEACOCK AND KENNETH P. DIAL

*Division of Biological Sciences, University of Montana, Missoula, MT 59812, USA*

\*Present address: Concord Field Station, Museum of Comparative Zoology, Harvard University, Old Causeway Road, Bedford, MA 01730, USA (e-mail: btobalske@oeb.harvard.edu)

*Accepted 5 April; published on WWW 8 June 1999*

### Summary

It has been proposed elsewhere that flap-bounding, an intermittent flight style consisting of flapping phases interspersed with flexed-wing bounds, should offer no savings in average mechanical power relative to continuous flapping unless a bird flies 1.2 times faster than its maximum range speed ( $V_{mr}$ ). Why do some species use intermittent bounds at speeds slower than  $1.2V_{mr}$ ? The ‘fixed-gear hypothesis’ suggests that flap-bounding is used to vary mean power output in small birds that are otherwise constrained by muscle physiology and wing anatomy to use a fixed muscle shortening velocity and pattern of wing motion at all flight speeds; the ‘body-lift hypothesis’ suggests that some weight support during bounds could make flap-bounding flight aerodynamically advantageous in comparison with continuous flapping over most forward flight speeds. To test these predictions, we studied high-speed film recordings (300 Hz) of wing and body motion in zebra finches (*Taenopygia guttata*, mean mass 13.2 g,  $N=4$ ) taken as the birds flew in a variable-speed wind tunnel ( $0\text{--}14\text{ m s}^{-1}$ ). The zebra finches used flap-bounding flight at all speeds, so their flight style was unique compared with that of birds that facultatively shift from continuous flapping or flap-gliding at slow speeds to flap-bounding at fast speeds. There was a significant effect of flight speed on all measured aspects of wing motion except percentage of the wingbeat spent in downstroke. Changes in angular velocity of the wing indicated that contractile velocity in the pectoralis muscle changed with flight speed, which is not consistent with the fixed-gear hypothesis. Although variation in stroke-plane angle relative to the body, pronation angle of the wing and wing span at mid-upstroke showed that the zebra finch changed within-

wingbeat geometries according to speed, a vortex-ring gait with a feathered upstroke appeared to be the only gait used during flapping. In contrast, two small species that use continuous flapping during slow flight ( $0\text{--}4\text{ m s}^{-1}$ ) either change wingbeat gait according to flight speed or exhibit more variation in stroke-plane and pronation angles relative to the body. Differences in kinematics among species appear to be related to wing design (aspect ratio, skeletal proportions) rather than to pectoralis muscle fiber composition, indicating that the fixed-gear hypothesis should perhaps be modified to exclude muscle physiology and to emphasize constraints due to wing anatomy. Body lift was produced during bounds at speeds from 4 to  $14\text{ m s}^{-1}$ . Maximum body lift was 0.0206 N (15.9% of body weight) at  $10\text{ m s}^{-1}$ ; body lift:drag ratio declined with increasing air speed. The aerodynamic function of bounds differed with increasing speed from an emphasis on lift production ( $4\text{--}10\text{ m s}^{-1}$ ) to an emphasis on drag reduction with a slight loss in lift ( $12$  and  $14\text{ m s}^{-1}$ ). From a mathematical model of aerodynamic costs, it appeared that flap-bounding offered the zebra finch an aerodynamic advantage relative to continuous flapping at moderate and fast flight speeds ( $6\text{--}14\text{ m s}^{-1}$ ), with body lift augmenting any savings offered solely by flap-bounding at speeds faster than  $7.1\text{ m s}^{-1}$ . The percentage of time spent flapping during an intermittent flight cycle decreased with increasing speed, so the mechanical cost of transport was likely to be lowest at faster flight speeds ( $10\text{--}14\text{ m s}^{-1}$ ).

Key words: zebra finch, *Taenopygia guttata*, kinematics, flap-bound, intermittent flight, aerodynamics, muscle, power output, efficiency, gait, lift, drag, flight.

### Introduction

Flap-bounding flight consists of flapping phases alternating with flexed-wing bounding phases; it is a style of locomotion commonly exhibited by many species of relatively small birds. Flapping phases alternate with extended-wing glides in flap-gliding flight. Both flap-bounding and flap-gliding are forms of intermittent flight. Recent studies in laboratory and field

settings have demonstrated that some bird species tend to use flap-gliding when flying slowly and shift towards the use of flap-bounding when flying at faster speeds (Tobalske and Dial, 1994, 1996; Tobalske, 1995, 1996). This shift in flight behavior according to flight speed probably offers an energetic saving in comparison with continuous flapping. Several mathematical

models of intermittent flight indicate that, in comparison with continuous flapping, flap-gliding should require less mechanical power output at slow speeds (Ward-Smith, 1984b; Rayner, 1985), and flap-bounding should require less mechanical power output at fast speeds (Lighthill, 1977; Rayner, 1977, 1985; Alexander, 1982; Ward-Smith, 1984a,b). Savings in mechanical power are probably important to many bird species, given the high metabolic cost of flapping per unit time (Goldspink, 1981).

Problems emerge when specific predictions are made regarding the flight speeds for which flap-bounding should offer an aerodynamic advantage (savings in average mechanical power output) to a bird, primarily because the authors presenting the existing models differ in their assumptions about largely unmeasured aspects of the kinematics and aerodynamics of flap-bounding. Using continuous flapping as a reference, power savings are variously predicted at most forward flight speeds (4–14 m s<sup>-1</sup>; DeJong, 1983), at forward flight speeds greater than or equal to the minimum power speed ( $V_{mp}$ ; Ward-Smith, 1984a,b) or at particularly fast flight speeds exceeding the maximum range speed ( $V_{mr}$ ; Lighthill, 1977; Rayner, 1977, 1985; Alexander, 1982).

As noted by Rayner (1985), the prediction that flap-bounding birds must exceed  $V_{mr}$  to gain an aerodynamic advantage is perplexing because  $V_{mr}$  is expected to be the optimal speed for migration, and small birds frequently engage in flap-bounding during migration (e.g. Pye, 1981; Danielson, 1988). Moreover, some bird species, including the zebra finch (*Taenopygia guttata*), engage in flap-bounding at slow flight speeds (0–6 m s<sup>-1</sup>; Csicsáky, 1977a,b; Scholey, 1983; Rayner, 1985).

Two parameters may explain the observed discrepancy between bird behavior and the prediction that flap-bounding birds must fly faster than  $V_{mr}$  to experience an aerodynamic advantage: a ‘fixed-gear’ may be present in the flight apparatus of birds that use flap-bounding at all flight speeds (Goldspink, 1977; Rayner, 1977, 1985; Ward-Smith, 1984b), and the production of an upwardly directed lifting force (‘body-lift’) during bounds could make flap-bounding aerodynamically advantageous even at moderate flight speeds including  $V_{mr}$  (Csicsáky, 1977a,b; Rayner, 1985). We will briefly introduce these two parameters in the form of two hypotheses.

#### *Fixed-gear hypothesis*

The fixed-gear hypothesis predicts that a size-based constraint on the heterogeneity of fiber types in the pectoralis muscle (the primary downstroke muscle in birds) restricts small birds to a single, fixed level of power output per wingbeat (Goldspink, 1977; Rayner, 1977, 1985; Ward-Smith, 1984b). For small birds, the hypothesis suggests that variation in contractile velocity from an optimum velocity would result in a serious loss of efficiency and power output during the conversion of chemical energy into mechanical work, and fixed motor-unit recruitment patterns restrict variation in force production. This reasoning has its origins in the classic work

of Hill (1950) and remains a current area of inquiry (Barclay, 1996; Askew and Marsh, 1998).

Secondly, the fixed-gear hypothesis predicts that, because of anatomical constraints associated with wing design, flap-bounding birds lack the ability to change wingbeat kinematics or wingbeat gaits to accommodate optimally the aerodynamic demands of flight over a wide range of speeds (Rayner, 1985). Azuma (1992) suggested that skeletal proportions in flap-bounding birds may limit variation in wing span and area among flight speeds; otherwise, no specific anatomical features of the wing have been proposed as functional constraints on variation.

Gaits in avian flight are currently characterized using the aerodynamic function of the upstroke, and kinematics may be used to infer gait selection (Rayner, 1991; Tobalske and Dial, 1996). Two types of vortex-ring gait are known: feathered upstroke and tip-reversal upstroke. During a feathered upstroke (Bilo, 1972), the entire wing is highly flexed, and it is reported that lift is produced only during the downstroke (Kokshaysky, 1979). During a wingtip-reversal upstroke (Brown, 1963), the wing is only partially flexed, and the distal wing is supinated. The upstroke may be aerodynamically active as a result of profile drag on the wing (Warrick and Dial, 1998), but vortex-visualization studies suggest that no lift is produced (Rayner, 1991). In contrast with the vortex-ring gait, in the continuous-vortex gait, the wings are relatively extended and produce lift during the upstroke (Spedding, 1987; Rayner, 1991). Birds with long wings or wings of high aspect ratio tend to use a vortex-ring gait with a tip-reversal upstroke at slow speeds and a continuous-vortex gait at fast speeds (Scholey, 1983; Rayner, 1991; Tobalske and Dial, 1996).

To summarize, rather than varying muscle power and wingbeat kinematics with flight speed as larger birds do (Tobalske and Dial, 1996; Dial et al., 1997), small flap-bounding birds are predicted to have a fixed wingbeat ‘gear’ optimized for ascending flight, perhaps with acceleration or added payload, and they vary mean power output below this fixed maximum solely using intermittent bounds (Rayner, 1977, 1985; Ward-Smith, 1984b; Azuma, 1992).

Aspects of the fixed-gear hypothesis are not supported by kinematic and electromyographic data obtained from the budgerigar (*Melopsittacus undulatus*), a species that uses continuous flapping during hovering (Scholey, 1983) and engages in both flap-gliding and flap-bounding during forward flight (7–16 m s<sup>-1</sup>; Tobalske and Dial, 1994). Although this species has only one fiber type in its pectoralis muscle (fast-twitch oxidative glycolytic, FOG, type R; Rosser and George, 1986), it has a body mass of 34.5 g and relatively long, pointed wings. The smallest species using flap-bounding measure 5 g or less (e.g. kinglets, *Regulus* spp.), and many have relatively rounded wings. It remains possible that the fixed-gear hypothesis applies to particularly small flap-bounding birds with wings of low aspect ratio. Kinematic data obtained from a single zebra finch (13 g; only FOG fibers in the pectoralis, type R or I, not specified; Rosser et al., 1996) hovering and flying at 5 m s<sup>-1</sup> are consistent with the fixed-gear hypothesis

(Scholey, 1983; Rayner, 1985). Wingbeat frequency and amplitude reportedly covary between the two flight speeds so that the velocity of the wing, and by inference the contractile velocity of the pectoralis, is estimated to be almost constant; the angle of the stroke plane relative to the body is virtually identical at the two speeds (Scholey, 1983). Similar data are not available for wingbeat kinematics at other flight speeds, or for variation among individuals.

#### Body-lift hypothesis

A body-lift hypothesis suggests that partial weight support during bounds would make flap-bounding aerodynamically attractive at intermediate and fast flight speeds. Using plaster casts of zebra finch bodies, Csicsáky (1977a,b) first demonstrated that air flowing over the body could generate an upwardly directed vertical force that was capable of supporting a percentage of body weight during the flexed-wing bound. Csicsáky (1977a,b) named this force body lift and identified as body drag the horizontal force during the bound that is directed in the opposite direction to the flight path. We retain these terms in the present investigation, although the flow characteristics responsible for the vertical force have not been documented and may result from pressure drag rather than vortex circulation (Rayner, 1985).

Csicsáky (1977a,b) argues that body lift is produced during bounds in the zebra finch because the percentage of time the finches spend flapping decreases with increasing flight speed up to a speed of  $6 \text{ m s}^{-1}$ . Unfortunately, these data do not provide adequate proof of body lift *in vivo*, because  $6 \text{ m s}^{-1}$  is an intermediate flight speed for a flap-bounding bird the size of the zebra finch (Rayner, 1979; DeJong, 1983; Azuma, 1992), and mechanical power is expected to vary with flight speed according to a U-shaped curve (Pennycuik, 1975; Rayner, 1979). The zebra finch may simply decrease the percentage of time spent flapping by virtue of mechanical power decreasing as speed increases, without generating body lift. Woicke and Gewecke (1978) mention that tethered siskins (*Carduelis spinus*) generate body lift during bounds, but do not report the magnitude of the force under these admittedly unusual flight conditions. Thus, evidence for body lift during flap-bounding is scant, with no empirical data on the magnitude of body lift or on how flight speed affects body lift and drag during bounds in living birds.

This paucity of data is unfortunate, because the contribution of body lift to overall weight support during flap-bounding flight may revise our interpretation of the aerodynamic advantages of the flight style. According to Rayner (1985), body lift during bounding phases can potentially make flap-bounding less costly than continuous flapping during flight at moderate speeds including  $V_{\text{mr}}$ . DeJong's (1983) model does not include body lift but does include an extremely brief glide at the end of the bound phase, and the glide angle achieved during this 'pull-out' from the bound is shown to make flap-bounding energetically attractive for a small bird at all flight speeds from 4 to  $14 \text{ m s}^{-1}$ .

#### Goals of the present study

Zebra finches were selected for this investigation because previous research (Csicsáky, 1977a,b; Scholey, 1983) suggested that the species should exhibit a fixed wingbeat gear and generate body lift during intermittent bounds, yet data were only available over a limited range of speeds or from plaster-cast models rather than living birds. We report on the wing and body kinematics of zebra finches flying in a wind tunnel at speeds from 0 to  $14 \text{ m s}^{-1}$ , the maximum range of speeds at which the birds would fly. We use these data to evaluate the assumptions made in existing aerodynamic models of flap-bounding flight and to test the predictions of the fixed-gear and body-lift hypotheses as they pertain to particularly small, flap-bounding birds.

### Materials and methods

#### Birds and training

Zebra finches *Taenopygia guttata* ( $N=4$ , female) were obtained from a commercial supplier. All bird training and subsequent experimentation were conducted in Missoula, MT, USA, at an altitude of 970 m above sea level,  $46.9^\circ$  latitude; for this location, gravitational acceleration is  $9.8049 \text{ m s}^{-2}$  and average air density is  $1.115 \text{ kg m}^{-3}$  (Lide, 1998). Morphometric data were collected from the birds immediately after conducting the experiments (Table 1). Body mass (g) was measured using a digital balance. Wing measurements were made with the wings spread as during mid-downstroke, with the emargination on the distal third of each of the primaries completely separated from adjacent feathers. These data included the wing span (mm) between the distal tips of the ninth primaries, the wing length (mm) from the shoulder joint to the distal tip of the ninth primary, the surface area of a single wing ( $\text{cm}^2$ ) and the combined surface area of both wings and the portion of the body between the wings ( $\text{cm}^2$ ). Aspect ratio was computed as the square of wing span divided by combined surface area. Wing loading ( $\text{N m}^{-2}$ ) was body

Table 1. *Morphological data for the zebra finch (Taenopygia guttata)*

Variable	Mean value
Body mass (g)	13.2±0.9
Wing span (mm)	169.3±1.7
Wing length (mm)	74.8±0.6
Distance between shoulders (mm)	19.7±0.5
Single wing surface area ( $\text{cm}^2$ )	28.6±0.9
Both wings and body surface area ( $\text{cm}^2$ )	63.4±1.7
Wing aspect ratio	4.5±0.1
Wing loading ( $\text{N m}^{-2}$ )	20.5±1.5
Tail area ( $\text{cm}^2$ )	8.8±0.9
Total length (mm)	102.0±1.9

Values are means  $\pm$  S.E.M.,  $N=4$ .

Measurements were made with the wings spread as in mid-downstroke and tail spread to  $50^\circ$ .

weight divided by combined area. The surface area of the tail ( $\text{cm}^2$ ), cranial to the maximum continuous span (Thomas, 1993), was measured with the tail spread so that the acute angle described between the vanes of the outermost retrices was approximately  $50^\circ$ . Wing span (mm) and total length (mm) were obtained using a metric rule. All measurements of surface area were obtained by tracing an outline of the bird on millimeter-rule graph paper, video-taping the outline and transferring the images to a computer for subsequent digitizing and analysis.

The birds were trained to fly within the flight chamber of a wind tunnel using the same methods previously employed in studies of intermittent flight in birds at the University of Montana (Tobalske and Dial, 1994, 1996; Tobalske, 1995). Each zebra finch was trained for approximately 30 min per day to fly at wind-tunnel air speeds from 0 to  $14 \text{ m s}^{-1}$ , the maximum range over which we could encourage all the birds to fly. The zebra finches were considered to be ready for the experiments when the birds would sustain 1–3 min of flight at moderate and fast wind-tunnel speeds ( $4\text{--}14 \text{ m s}^{-1}$ ) and 10–30 s of flight at slow speeds ( $0\text{--}2 \text{ m s}^{-1}$ ).

#### Wind tunnel

The wind-tunnel flight chamber measured  $76 \text{ cm} \times 76 \text{ cm} \times 91 \text{ cm}$  and had clear acrylic walls (6.3 mm thick) to provide an unobstructed view for filming. Air was drawn through the flight chamber by a fan coupled to a variable-speed d.c. motor. Three turbulence-reducing baffles (5 mm honeycomb, 10 cm thick) were installed upwind from the flight chamber in the contraction cone. One baffle was located at the inlet of the cone, the other two downwind, adjacent to the flight chamber. Contraction ratio was 2.8:1. Airflow was laminar in all areas of the flight chamber more than 2.5 cm from the walls, and the velocity of the airflow varied by no more than 4.2% (Tobalske and Dial, 1994). Wind velocities were monitored using a Pitot tube and airspeed indicator calibrated with an electronic airspeed indicator.

#### Kinematics

Zebra finch flights within the wind tunnel were filmed using a Red Lakes 16 mm camera at  $300 \text{ frames s}^{-1}$ , with an exposure time of 1.11 ms per frame (effective shutter opening of  $120^\circ$ ). Simultaneous lateral and dorsal views of the zebra finch were obtained by placing the camera lateral to the flight chamber and using a mirror mounted at  $45^\circ$  on top of the flight chamber. Some flights were filmed using a narrower field of view for enhanced detail, which provided either a lateral or dorsal view of a bird. Flights during experiments were 10 s or longer in duration, with filming periods lasting approximately 5 s. Between flights, the bird rested on a removable perch and speed was changed in the wind tunnel. The order of flight speeds during experiments was randomly assigned for each bird.

Film was viewed using a motion-analyzer projector with a frame counter. Flights ( $N=34$ ) were divided into separate 'cycles' consisting of a flapping phase followed by a non-

flapping phase ( $N=555$ ). Non-flapping intervals consisted of bounds during which the wings were held motionless and flexed against the body for periods of 10 ms or more (minimum of three frames at 300 Hz). Rarely, three of the zebra finches performed intermittent glides ( $N=5$ ), with the wings held extended and motionless; these sporadic cycles were noted but excluded from summaries and statistical analysis of the flap-bounding data. Using frame counts (each frame represented 3.33 ms), we measured the duration of the flapping phase (ms), the duration of the bounding phase (ms) and, from these two variables, we calculated the percentage of the cycle time spent flapping (%). The number of wingbeats within each flapping phase was counted, and this number was divided by the duration of the flapping phase (in s) to provide our measure of wingbeat frequency (Hz).

The kinematics were further examined by projecting each frame of film onto a graphics tablet and digitizing anatomical landmarks. These included the distal tip of the beak, the eye (=center of head), the base of the tail at the midline of the body, the distal tip of the tail, the distal tips of the wings at the ninth primary feather and (from a lateral view of mid-downstroke only) the mid-line leading edge of the wing and the mid-line trailing edge of the wing. Vertical and horizontal reference points on the walls of the flight chamber were also digitized. Digitized points were acquired using NIH Image 1.6 software (National Institutes of Health). The  $x$ - $y$  pixel coordinates were converted into metric distance using two known measures on a given bird as a scale: body length from the distal tip of the beak to the distal tip of the tail, and wing span at mid-downstroke (Table 1). The pixel-to-metric distance conversion, and all subsequent kinematic analyses, were conducted using Microsoft Excel v.4.0 (Microsoft, Inc.) and a Power Macintosh 6500 computer.

Within-wingbeat kinematics (Fig. 1) were obtained from randomly selected wingbeats ( $N=20$ ) for each bird at each speed. Wing span (mm) was the instantaneous distance between the distal tips of the wings at the ninth primary, measured from a dorsal view. Wingtip elevation (mm) was the perpendicular distance from the distal tip of the wing at the ninth primary to the lateral midline, with the lateral midline described by the points on the center of the head (eye) and the lateral base of the tail (Fig. 1A). Wingbeat amplitude (degrees) was converted from wingtip elevation using the formula:

$$WA = \tan^{-1} \left( \frac{WE_a}{0.5(B_a - X)} \right) + \tan^{-1} \left[ \left( \frac{WE_b}{0.5(B_b - X)} \right) \right] \quad (1)$$

where  $WA$  is wingbeat amplitude,  $WE_a$  is wingtip elevation at the start of downstroke,  $WE_b$  is wingtip elevation at the end of downstroke,  $B_a$  is wing span at the start of downstroke,  $B_b$  is wing span at the end of downstroke and  $X$  is the distance between the shoulder joints. The angular velocity of the wing ( $\text{degrees ms}^{-1}$ ) was obtained by dividing total wing amplitude by downstroke duration (ms); flapping velocity ( $V_f$ ;  $\text{m s}^{-1}$ ) for any chord along the length of the wing was calculated by

multiplying angular velocity ( $\text{rad s}^{-1}$ , converted from degrees  $\text{ms}^{-1}$ ) by length (m) from the wing chord to the base of the wing. The angle of incidence of the wing ( $\alpha$ ; degrees; often called the angle of attack, relative to incident air) was calculated as the angle between the wing chord (defined by the midline of the leading and trailing edges of the wing) and relative airflow was defined by the resultant vector of added vectors representing  $V_i$ , body velocity ( $V$ ) and the vertical component of induced velocity ( $V_i$ ; Aldridge, 1986; Fig. 1B). Herein, we report the angle of incidence for the chord halfway along the length of the wing (37.4 mm from the shoulder; Table 1) that was visible in lateral view at mid-downstroke (Fig. 1B). As the avian wing is flexible, the angle of incidence varies along the length of the wing in a complex manner (Bilo, 1971), so our measure should not be interpreted as representing the angle of incidence at other lengths along the wing. We used the Rankine–Froude momentum theory of propellers to estimate the vertical component of induced velocity ( $V_i$ ;

Pennycuick, 1975; Aldridge, 1986), the vector sum of bound and wake vortices. During hovering:

$$V_i = \left( \frac{W}{2\rho S_d} \right)^{0.5}, \quad (2)$$

where  $W$  is body weight (N),  $\rho$  is air density ( $\text{kg m}^{-3}$ ) and  $S_d$  is the disk area of the wings ( $\text{m}^2$ ); i.e. the area of a circle with a diameter equal to the wing span at mid-downstroke (Table 1). During forward flight:

$$V_i = \left( \frac{W}{2V\rho S_d} \right), \quad (3)$$

where  $V$  is body velocity. During slow flight, wake-induced velocity is high and our estimate of  $V_i$  is therefore likely to be inaccurate (Rayner, 1979; Aldridge, 1986). Thus, caution is required when interpreting the angles of incidence we report for slow flight speeds ( $0\text{--}4 \text{ m s}^{-1}$ ). Body angle  $\beta$  was measured as the angle formed by the lateral midline of the body and a horizontal reference line (Fig. 1B). Pronation angle  $\phi$  was the angle between the lateral midline of the body and the wing chord halfway along the length of the wing. Stroke plane was defined by a lateral line connecting the tip of the ninth primary at the beginning and at the end of downstroke; using this variable, we computed stroke-plane angle relative to the midline of the body  $\delta_b$  and relative to a horizontal reference  $\delta_h$  (Fig. 1A).

Vertical and horizontal forces acting on the body of the zebra finch during bounds ( $N=183$ ) were calculated using measures of acceleration (Fig. 2) according to the standard formula expressing Newton's second law of motion wherein force (N) is equal to mass (kg; Table 1) multiplied by acceleration ( $\text{m s}^{-2}$ ). Position during the bound was represented by the  $x$  (=horizontal) and  $y$  (=vertical) coordinates of the zebra finch eye in units of metric distance. To obtain vertical acceleration, the  $y$ -coordinate data were plotted as a function of time, and a second-order polynomial curve was fitted to the data (Cricket Graph III, v.1.5.1; Computer Associates International, Inc.). The second derivative of the equation for the line describing the curve yielded the magnitude of a resultant acceleration vector directed towards earth (arbitrarily assigned a negative direction). We solved for the magnitude of the upwardly directed component vector contributing to this resultant by subtracting the component due to gravitational acceleration ( $=-9.8049 \text{ m s}^{-2}$ ). Horizontal acceleration was measured using  $x$ -coordinate data and the same methods, with the exception that the resultant horizontal acceleration directed in the opposite direction to the flight path of the bird was arbitrarily assigned a positive value and there was no component of gravity in this dimension.

Body angle  $\beta$ , between the lateral midline of the body and a horizontal reference line, was measured during all bounds.

We excluded from subsequent analysis all bounds shorter than 33 ms in duration (10 frames of film), because the curves fitted to the position data for these short intervals were overly sensitive

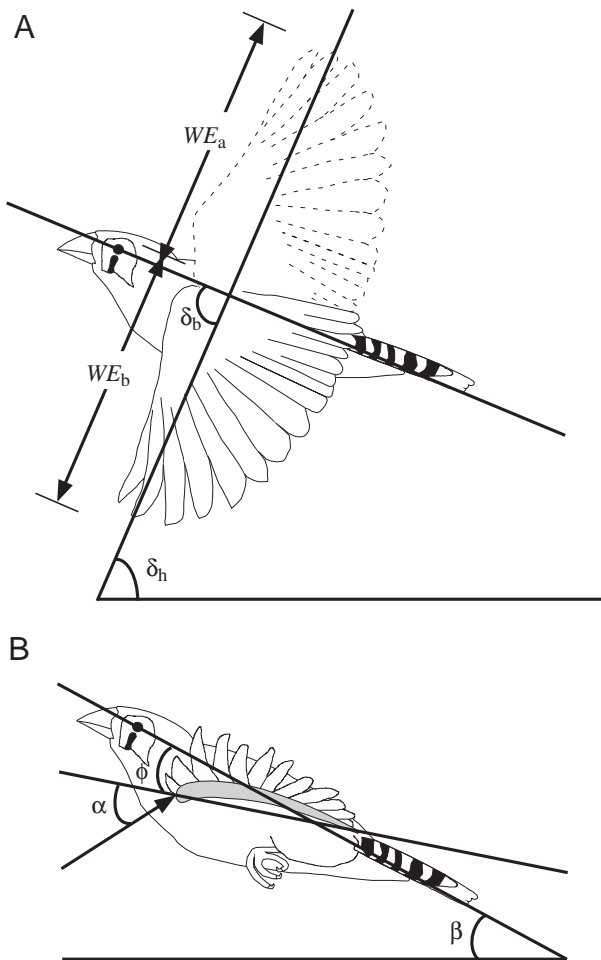


Fig. 1. Wing and body kinematics measured from flying zebra finches (*Taenopygia guttata*). (A)  $WE_a$ , wingtip elevation at the start of downstroke;  $WE_b$ , wingtip elevation at the end of downstroke;  $\delta_b$ , stroke-plane angle relative to the body;  $\delta_h$ , stroke-plane angle relative to horizontal. (B)  $\phi$ , pronation angle of the wing;  $\alpha$ , angle of incidence of the wing;  $\beta$ , body angle relative to horizontal.

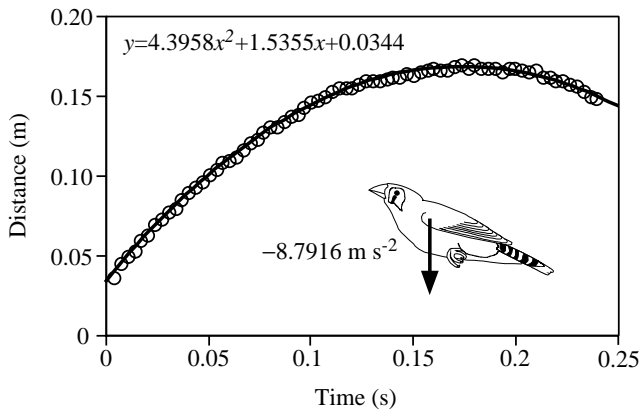


Fig. 2. Method used to calculate body lift and drag during a bound in a zebra finch (*Taenopygia guttata*). Vertical acceleration during the bound was measured by taking the second derivative of a second-order polynomial equation for a curve fitted to digitized points representing the position of the zebra finch eye (center of head) as a function of time. In this instance, from a zebra finch (ZF3) flying at  $6 \text{ m s}^{-1}$ , vertical acceleration was  $-8.7916 \text{ m s}^{-2}$  (negative sign arbitrarily assigned), indicating that an upwardly directed acceleration of  $1.0133 \text{ m s}^{-2}$  was opposing acceleration due to gravity ( $-9.8049 \text{ m s}^{-2}$ ). Multiplying the upward acceleration by body mass ( $0.0132 \text{ kg}$ ) indicated an upwardly directed vertical force (body lift) of  $0.0136 \text{ N}$ , supporting 10.3% of body weight. Horizontal force (body drag) was calculated using horizontal position as a function of time (not shown).

to outliers, yielded low  $r$  values and indicated clearly spurious values. This precluded the analysis of accelerations during all bounds at  $0 \text{ m s}^{-1}$  and a limited number of bounds at other speeds.

#### Statistical analyses

Values are presented as means  $\pm$  S.E.M. ( $N=4$  zebra finches). For each of the variables examined in this study, we computed the mean value within each bird at each speed ( $N=8$ ). The distributions of these mean values did not violate assumptions associated with parametric statistical analysis; thus, we tested for a significant effect of flight speed upon each variable using univariate repeated-measures analysis of variance (von Ende, 1993; MANOVA procedure, SPSS for the Macintosh, v.4.0, SPSS, Inc).

### Results

The zebra finches used flap-bounding flight at all speeds ( $0\text{--}14 \text{ m s}^{-1}$ ; Fig. 3). Sporadic intermittent glides ( $N=5$ , 0.9% of the total number of flap-bounding cycles) were exhibited by three birds (also observed by Csicsáky, 1977a). These glides did not appear to be associated with a particular flight speed and they were not included in the present analyses.

#### Within-wingbeat kinematics

There was a significant effect of flight speed on every variable describing the wing and body kinematics during flapping in the zebra finch except the percentage of the

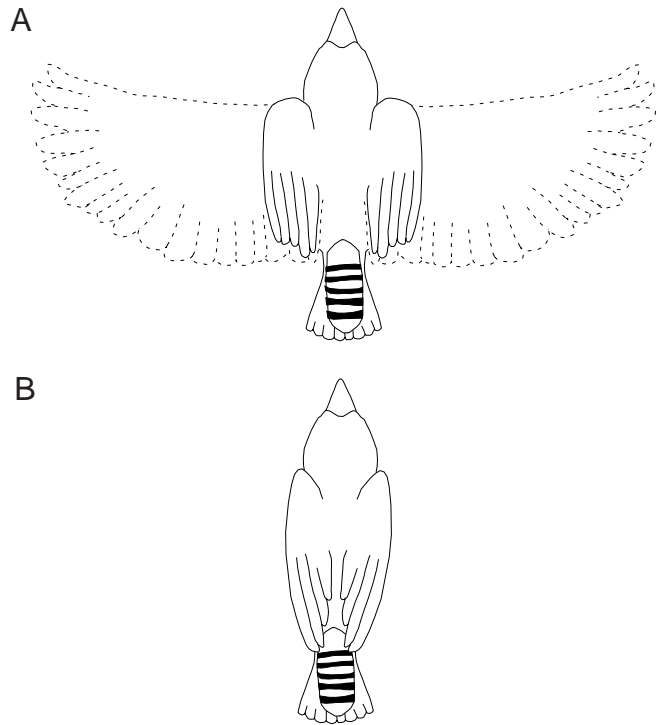


Fig. 3. Dorsal views of wing and body posture in a zebra finch (*Taenopygia guttata*; ZF2) engaged in flap-bounding flight at  $8 \text{ m s}^{-1}$ . (A) Flapping phase, with wing posture at mid-downstroke (dashed line) and at mid-upstroke (solid line). (B) Bounding phase, with the wings fully flexed.

wingbeat spent in downstroke (Table 2). Wingbeat frequency showed a gradual trend to increase with increasing flight speed (Table 2; Fig. 4) and, because the percentage of the wingbeat cycle spent in the downstroke was approximately 60% at all speeds, the absolute duration of the downstroke decreased with increasing speed. Wingbeat amplitude decreased with increasing flight speed (Fig. 4B). Frequency and amplitude did not change so as to maintain a fixed angular velocity of the wing. The angular velocity of the wing was highest during hovering, decreased to a minimum at a flight speed of  $8 \text{ m s}^{-1}$ , and increased slightly with each further increase in flight speed up to  $14 \text{ m s}^{-1}$  (Table 2; Fig. 4).

Three other measures provide insight into wing motion in relation to the body. Stroke-plane angle relative to the body varied between  $81.7$  and  $91.8^\circ$ , with higher values exhibited at intermediate flight speeds. Likewise, wing span at mid-upstroke tended to be higher at intermediate flight speeds, reaching a maximum of  $37.4 \text{ mm}$ , or 22.1% of mean downstroke span, during flight at  $10 \text{ m s}^{-1}$  (Table 2). Finally, the pronation angle of the wing decreased as flight speed increased.

As mean wing span at mid-upstroke did not exceed 22.1% of mean downstroke span, and the wings were highly flexed and pronated at mid-upstroke (Table 2; Fig. 3A), it appeared that the zebra finch used a vortex-ring gait with a feathered upstroke at all flight speeds (Bilo, 1972; Kokshaysky, 1979; Tobalske and Dial, 1996).

Body angle in relation to the horizontal decreased continuously as speed increased (Table 2). This pattern, together with the changes in wing motion relative to the body mentioned above, resulted in changes in wing motion relative to the laboratory coordinate space (distinct from changes defined by the coordinates of the bird's body). As speed increased, stroke-plane angle relative to horizontal increased, whereas the angle of incidence of the wing decreased.

*Flap-bounding kinematics*

The percentage of time that a zebra finch spent flapping during a cycle of flap-bounding flight decreased as a function of airspeed (repeated-measures ANOVA; d.f., 21,7;  $F=35.5$ ;  $P<0.0005$ ; Fig. 5A). This change was the result of a significant decrease in the duration of flapping phases ( $F=7.4$ ;  $P<0.0005$ ) and a significant increase in the duration of bounding phases ( $F=19.4$ ;  $P<0.0005$ ) as flight speed increased (Fig. 5B). The number of wingbeats within a flapping phase also changed significantly ( $F=4.9$ ;  $P=0.002$ ) with flight speed (Fig. 5C), reaching a maximum during hovering and a minimum during flight at  $6\text{ m s}^{-1}$ .

To describe the overall patterns of flap-bounding flight in

the zebra finch, we present kinematic data during 1 s of flight exhibited by a zebra finch (ZF1) flying at 2 and  $12\text{ m s}^{-1}$  (Fig. 6). Patterns of wing span and wingtip elevation clearly revealed the decrease in the percentage of time spent flapping as flight speed increased. However, certain aspects were similar at both speeds. There was considerable variation in the number of wingbeats within flapping phases at both flight speeds, with 2–8 wingbeats per flapping phase at  $2\text{ m s}^{-1}$  and 3–6 wingbeats per cycle at  $12\text{ m s}^{-1}$ . Wing span during bounds was always less than wing span at mid-upstroke during flapping phases (see also Fig. 3), and the wingtips were always held near the lateral midline of the body during bounds. Within-wingbeats, wing span was maximal at mid-downstroke and minimal at mid-upstroke. Lastly, some variation in wingtip elevation was observed within flapping phases. For example, in the second flapping phase in Fig. 6B, six wingbeats are represented. The first two wingbeats exhibit less excursion than wingbeats 4 and 5 in the same flapping phase.

During bounds, just as for flapping phases (Table 2), the mean body angle relative to horizontal decreased significantly as flight speed increased (repeated-measures ANOVA; d.f., 21,7;  $F=54.2$ ;  $P<0.0005$ ; Fig. 7). In every bound observed in

Table 2. Wing and body kinematics during flapping phases of flap-bounding flight in the zebra finch (*Taenopygia guttata*)

Variable	Flight speed ( $\text{m s}^{-1}$ )								F	P
	0	2	4	6	8	10	12	14		
Wingbeat frequency (Hz)	24.1±0.7	23.7±0.6	24.9±1.2	24.3±1.5	24.8±1.1	26.5±0.6	26.9±0.7	26.8±0.5	4.4	0.004*
Downstroke (%)	58.1±1.6	61.4±1.1	60.3±0.8	62.4±1.6	60.4±1.5	59.4±1.0	59.8±1.7	58.0±0.7	2.0	0.122
Downstroke duration (ms)	18.7±0.6	20.0±1.0	18.4±1.2	19.0±1.4	18.4±0.9	17.3±0.8	16.3±0.7	15.5±0.5	9.8	<0.0005*
Wing amplitude (degrees)	134.2±7.6	114.0±3.3	112.2±4.2	104.1±4.5	93.3±4.5	91.9±8.9	88.4±5.7	89.6±3.5	22.6	<0.0005*
Angular velocity of wing (degrees $\text{ms}^{-1}$ )	7.2±0.3	5.7±0.4	6.2±0.5	5.6±0.6	5.1±0.5	5.4±0.7	5.5±0.6	5.8±0.1	7.8	<0.0005*
Stroke-plane angle relative to horizontal (degrees)	33.3±3.2	45.7±3.8	55.3±2.6	61.6±2.5	65.7±1.8	70.1±1.6	72.4±1.4	72.2±2.2	80.8	<0.0005*
Stroke-plane angle relative to body (degrees)	81.7±0.7	85.0±1.2	91.8±2.4	91.0±2.8	90.4±3.2	90.9±2.5	86.5±2.7	85.0±2.8	7.0	<0.0005*
Pronation angle (degrees)	20.0±2.7	21.5±0.7	20.8±1.5	20.0±1.7	18.5±1.7	18.4±2.1	15.9±2.0	12.2±1.9	6.9	<0.0005*
Body angle (degrees)	48.6±3.6	39.3±3.1	36.6±3.5	29.4±0.5	24.7±2.4	20.9±1.8	14.1±1.8	12.8±1.4	410.8	<0.0005*
Angle of incidence (degrees)	75.3±2.3	58.5±1.5	47.7±3.1	34.5±2.0	25.9±2.3	20.0±2.1	13.7±1.7	14.6±1.7	107.4	<0.0005*
Wing span at mid-upstroke (mm)	28.0±2.6	26.9±2.0	26.6±1.7	32.4±4.0	36.6±5.0	37.4±5.7	33.4±4.3	30.4±3.0	3.9	0.007*

Values are means ± s.e.m. (N=4).

Significant effects of flight speed are marked with an asterisk (repeated-measures ANOVA, d.f. 21,7).

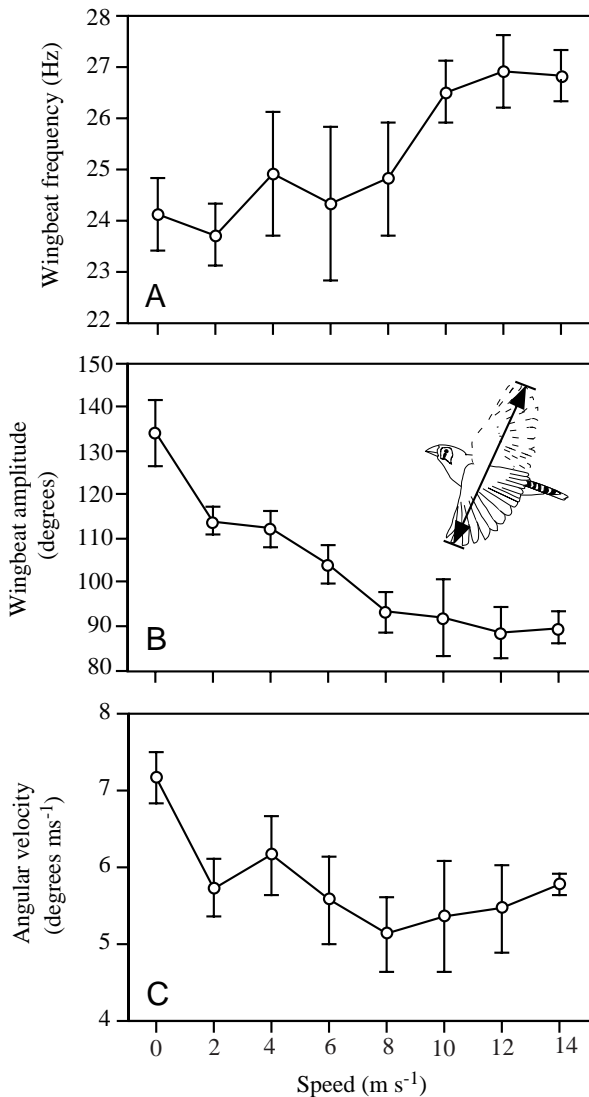


Fig. 4. Wingbeat frequency (A), wingbeat amplitude (B) and angular velocity of the wing during the downstroke (C) in four zebra finch (*Taenopygia guttata*) at flight speeds from 0 to 14 m s<sup>-1</sup>. Values are means  $\pm$  S.E.M.

this study ( $N=183$ ), the birds started the bound at a high body angle and decreased their body angle to reach a minimum value at the end of the bound. Usually, the variation in body angle relative to horizontal was over most of the range indicated by the dashed lines in Fig. 7. A typical example of this change in body angle and altitude in relation to a flap-bounding cycle is shown in Fig. 8 for a zebra finch (bird ZF3) flying at 12 m s<sup>-1</sup>. This portion of flight illustrates that body angle tended to increase during the latter portion of a flapping phase as the bird gained altitude, and then decreased during the bound as the bird's body described an arc trajectory as a function of time.

#### Body lift and drag

Body lift was generated during bounds at all forward flight speeds from 4 to 14 m s<sup>-1</sup> (Fig. 9A). There was a significant effect of speed on the magnitude of body lift (repeated-

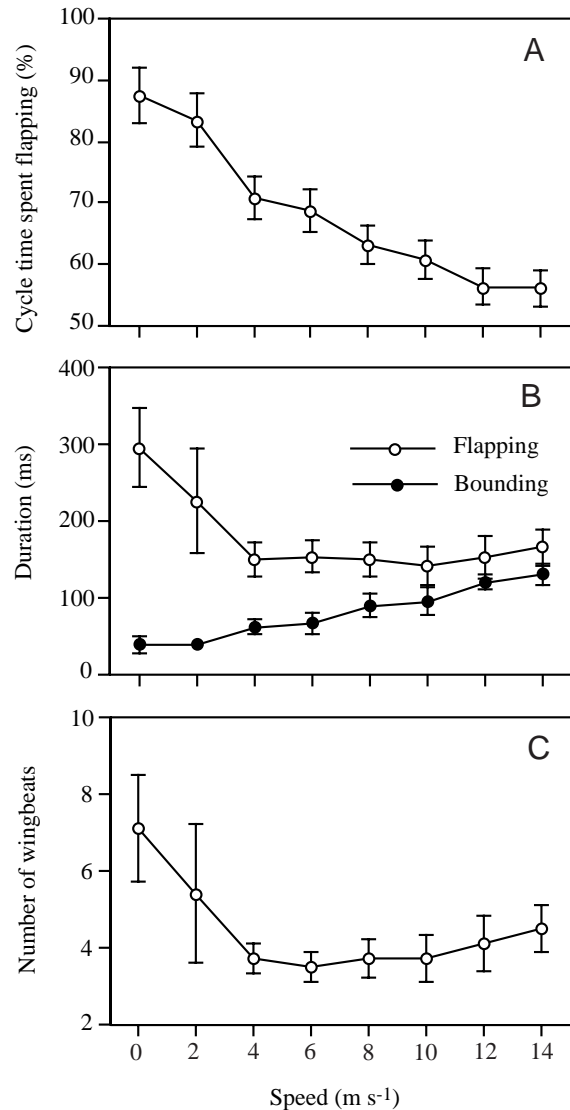


Fig. 5. Characteristics of flap-bounding flight in four zebra finches (*Taenopygia guttata*) at flight speeds from 0 to 14 m s<sup>-1</sup>. Values are means  $\pm$  S.E.M. (A) Percentage of time spent flapping in a flap-bounding cycle. (B) Duration of flapping and bounding intervals. (C) Number of wingbeats occurring in a flapping phase.

measures ANOVA; d.f. 21,6;  $F=6.9$ ;  $P=0.001$ ). Body lift was approximately 0N during bounds at 2 m s<sup>-1</sup>, and a maximum value of 0.0206N, representing 15.9% of body weight, was generated during bounds at 10 m s<sup>-1</sup> (Fig. 9A). Body drag also exhibited a significant change with flight speed (repeated-measures ANOVA; d.f. 21,6;  $F=8.8$ ;  $P<0.0005$ ) and reached a maximal value of 0.0158N during bounds at 10 m s<sup>-1</sup> (Fig. 9B). Virtually no body drag was detected during bounds at 2 m s<sup>-1</sup>.

Dividing body lift by body drag gives a lift:drag ratio for the body (Fig. 9C), which decreased with flight speed from 3.10 at 4 m s<sup>-1</sup> to 0.77 at 14 m s<sup>-1</sup>. These lift:drag ratios correspond to glide angles of 17.9 and 52.4°, respectively. The change in lift:drag ratio with speed, and the slight decrease observed in

both body lift and body drag as speed increased above  $10 \text{ m s}^{-1}$ , revealed that the zebra finches were changing the aerodynamic function of their bounds according to flight speed. Body lift appeared to be emphasized at slow speeds, particularly at  $4 \text{ m s}^{-1}$ , whereas the finches appeared to seek a reduction in body drag, at a slight expense to body lift, at  $12$  and  $14 \text{ m s}^{-1}$ .

### Discussion

#### Fixed-gear hypothesis

We infer that contractile velocity in the pectoralis changed according to flight speed, because there was a significant effect of flight speed on the angular velocity of the wing (Table 2; Fig. 4C). This result is not consistent with the prediction that small flap-bounding birds are restricted to a fixed level of power output per wingbeat (Rayner, 1977, 1985; Ward-Smith, 1984b). A comparison of the angular velocity of the wing at  $0$  and  $8 \text{ m s}^{-1}$  (Table 2; Fig. 4C) suggests that the contractile velocity in the pectoralis during maximal effort (i.e. hovering, climbing while accelerating or with added payload) is not identical to the contractile velocity during flight at intermediate speeds. For the zebra finches in our study, the angular velocity of the wing varied between  $5.1$  and  $7.2^\circ \text{ ms}^{-1}$ , an increase of  $39.9\%$ ; this is considerably greater than the  $5.1\%$  increase (from  $6.1$  to  $6.4^\circ \text{ ms}^{-1}$ ) exhibited by a zebra finch studied by Scholey (1983) flying at  $0$  and  $5 \text{ m s}^{-1}$  (our calculation from data given in Scholey, 1983).

The significant effects of flight speed on variables including stroke-plane and pronation angles relative to the body, and wing span at mid-upstroke, should similarly revise the assumption that flap-bounding birds must use wing-flapping geometries that are fixed in an absolute sense (Table 2). Among flight speeds, stroke-plane angle relative to the body increased by  $11.4\%$  (from  $81.7$  to  $91.8^\circ$ ), pronation angle relative to the body increased by  $76.2\%$  (from  $12.2$  to  $21.5^\circ$ ) and wing span at mid-upstroke increased by  $40.6\%$  (from  $26.6$  to  $37.4 \text{ mm}$ ). However, this variation occurred in what was apparently always a vortex-ring gait with a feathered upstroke (Table 2; Figs 3A, 6), and the use of only a single wingbeat gait represented less variation than if the zebra finch had changed between a vortex-ring and a continuous-vortex gait according to speed.

The biological significance of the observed variation should be evaluated in a comparative context, because it is possible that more variation in angular velocity of the wing or other wing kinematics, including a gait change, would be required to fly over the same range of speeds if the zebra finch did not use intermittent bounds. Ideally, comparisons should be made with species that use continuous flapping over a broad range of speeds; any differences in kinematics among species could be evaluated in relation to pectoralis composition and wing design. One current limitation is that it is not presently known whether the FOG fibers in the zebra finch pectoralis (Rosser et al., 1996) are exclusively type R or both types R and I. This merits study. An additional limitation is that more data are available for larger species (e.g. Scholey, 1983; Tobalske and Dial, 1996), but comparisons with larger species are not legitimate because of scaling effects. Negative scaling of available mass-specific power for flight (Pennycuik, 1975) or lift per unit power output (Marden, 1994) would mean that larger birds, by virtue of their size, should exhibit proportionally greater variation in wing kinematics to accomplish both hovering and cruising flight (Scholey, 1983).

An example explains this reasoning: comparing steady flight

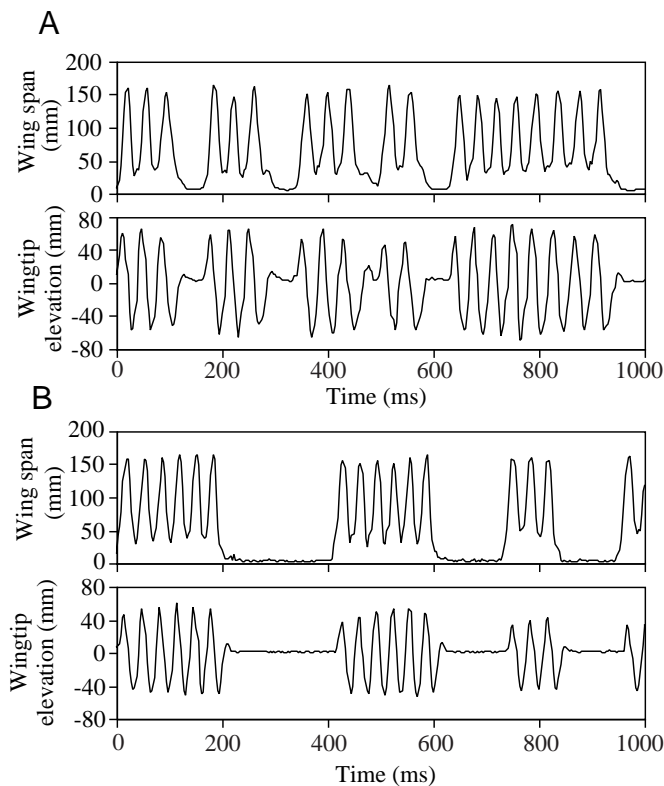


Fig. 6. Representative wing kinematics in a zebra finch (*Taenopygia guttata*, ZF1) engaged in flap-bounding flight at  $2 \text{ m s}^{-1}$  (A) and  $12 \text{ m s}^{-1}$  (B).

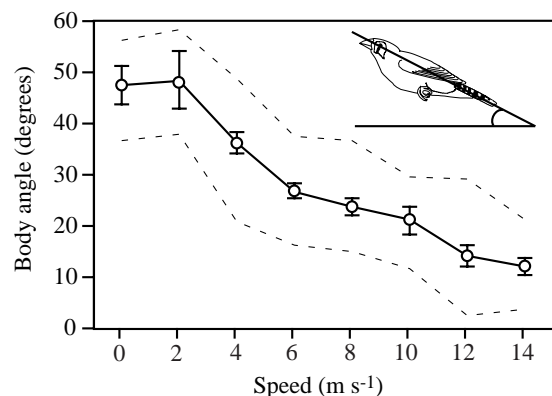


Fig. 7. Body angle relative to horizontal during bounding phases of flap-bounding flight in four zebra finches (*Taenopygia guttata*) at flight speeds from  $0$  to  $14 \text{ m s}^{-1}$ . Values are means  $\pm$  S.E.M. Dashed lines represent mean maximum angle and mean minimum angle exhibited during a bounding phase.

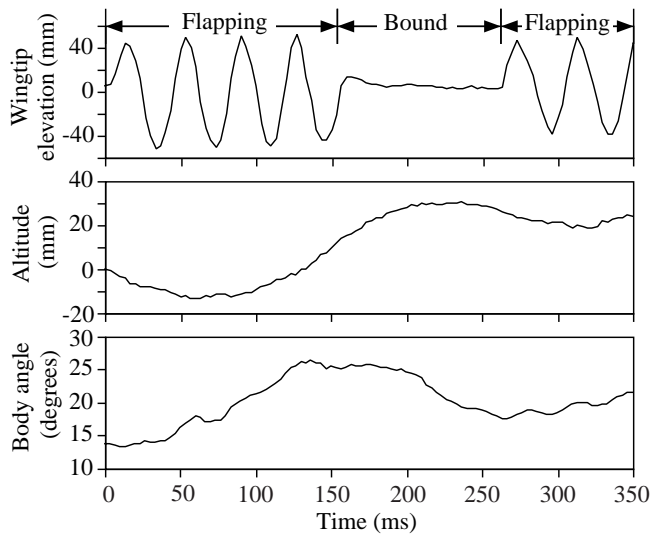


Fig. 8. Timing of a flap-bounding cycle in relation to changes in altitude and body angle in a zebra finch (*Taenopygia guttata*, ZF3) flying at  $12 \text{ m s}^{-1}$ .

at  $6.7 \text{ m s}^{-1}$  with hovering, the angular velocity of the wing increases by 111.1% (from  $0.7$  to  $1.6^\circ \text{ ms}^{-1}$ ) in the 158.3 g black-billed magpie (*Pica pica*; data from Tobalske and Dial, 1996; Tobalske et al., 1997). Although this species has only FOG fibers in its pectoralis, both types I and R are present (Tobalske et al., 1997). Because the black-billed magpie has the potential to recruit different fibers according to the contractile velocity required, and because it exhibits more variation in angular velocity of the wing than the zebra finch, the comparison suggests that the variation in angular velocity of the wing exhibited by the zebra finch was relatively small and, therefore, consistent with the fixed-gear hypothesis. However, because of its small size, it is not clear that the zebra finch would require a similar level of variation in angular velocity of the wing to fly at speeds from 0 to  $14 \text{ m s}^{-1}$  using continuous flapping.

We were able to study the flight kinematics of two small species that have wings of higher aspect ratio than those of the zebra finch (Table 1) and have pectoralis muscles consisting exclusively of type R fibers (Rosser and George, 1986). Values were obtained from our own calculations derived from quantitative data and illustrations of flight of the ruby-throated hummingbird (*Archilocus colubris*; 3 g, aspect ratio 8.1,  $N$  not known) in Greenewalt (1960; body mass from Dunning, 1993) and from our own analysis of video recordings ( $250 \text{ frames s}^{-1}$ ) of the budgerigar (34.5 g, aspect ratio 7.2,  $N=1$ ; video from M. Bundle and K. Dial, unpublished data). The ruby-throated hummingbirds flew in an open-section wind tunnel at 0, 4 and  $13 \text{ m s}^{-1}$ ; the budgerigar flew at speeds from 0 to  $18 \text{ m s}^{-1}$  in increments of  $2 \text{ m s}^{-1}$  in the same wind tunnel used in the present study. In each case, we consider maximum variation observed among speeds.

The ruby-throated hummingbird uses continuous flapping at all speeds and exhibits a 46.0% increase in angular velocity of

the wing (from  $8.8$  to  $12.8^\circ \text{ ms}^{-1}$ ) between  $4 \text{ m s}^{-1}$  and hovering. The budgerigar uses continuous flapping at slow speeds ( $0$ – $4 \text{ m s}^{-1}$ ) and intermittent flight at faster speeds ( $6$ – $18 \text{ m s}^{-1}$ ; also see Scholey, 1983; Tobalske and Dial, 1994); the angular velocity of the wing increases by 36.7% (from  $4.0$  to  $5.5^\circ \text{ ms}^{-1}$ ) between 10 and  $0 \text{ m s}^{-1}$ . Variation in angular velocity of the wing in both species is in the same range as that exhibited by the zebra finch (Table 2; Fig. 4). This provides comparative evidence that the zebra finch did not use a fixed contractile velocity in its pectoralis relative to species that do not use flap-bounding flight at slow speeds.

Substantial differences emerge among species when other wingbeat kinematics are examined. The ruby-throated hummingbird keeps its wings fully extended and uses wing

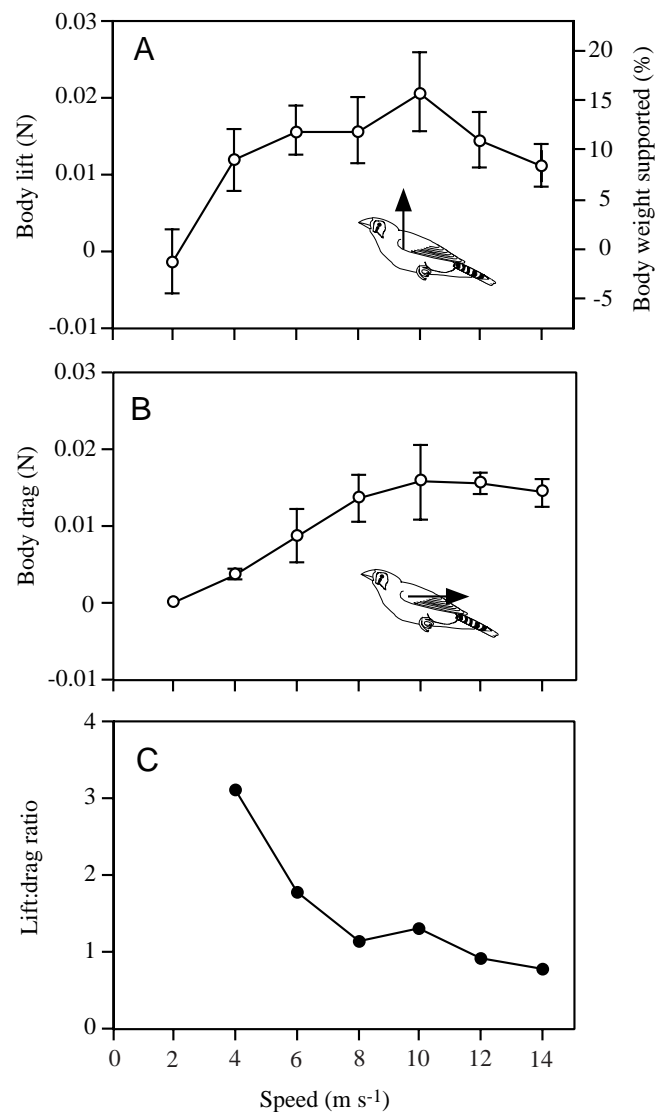


Fig. 9. Body lift (A), body drag (B) and lift:drag ratio (C) in four zebra finches (*Taenopygia guttata*) during the bounding phase of flap-bounding flight at wind-tunnel speeds from 2 to  $14 \text{ m s}^{-1}$ . Values are means  $\pm$  S.E.M., except for lift:drag ratio, which was computed from group means for body lift and drag, where only mean values are shown.

reversal during upstroke at all speeds, which requires almost  $180^\circ$  pronation and supination of the wing with each wingbeat. Stroke-plane angle relative to the body increases by 197.9% (from  $48$  to  $95^\circ$ ) between  $0$  and  $13\text{ m s}^{-1}$  (Greenewalt, 1960). The zebra finch showed considerably less variation in pronation and stroke-plane angle relative to the body (Table 2). Unlike the zebra finch (Figs 3A, 6), the budgerigar changes wingbeat gait. It uses a vortex-ring gait with wingtip reversal during slow flight ( $0\text{--}4\text{ m s}^{-1}$ ) and a continuous-vortex gait at faster speeds (Scholey, 1983; Tobalske and Dial, 1994). More similar to the variation exhibited by the zebra finch, however, the stroke-plane angle relative to the body in the budgerigar increases by 17.1% (from  $76.8$  to  $89.9^\circ$ ) between  $0$  and  $12\text{ m s}^{-1}$ , and the pronation angle increases by 65.5% (from  $7.7$  to  $12.8^\circ$ ) between  $18$  and  $10\text{ m s}^{-1}$ .

As the zebra finch, ruby-throated hummingbird and budgerigar all have only FOG fibers in their pectoralis muscles (Rosser and George, 1986; Rosser et al., 1996), the differences in kinematics among species are more clearly related to wing anatomy than to pectoralis muscle fiber composition. Hummingbirds have an unusual shoulder joint that permits a large range of motion relative to that available to other birds (Greenewalt, 1960), and their distal wing bones are proportionally longer than those in passerines (Dial, 1992). Both the hummingbird and the budgerigar have wings of higher aspect ratio than those of the zebra finch and, in birds other than hummingbirds, having pointed wings or wings of high aspect ratio is generally associated with wingtip reversal during slow flight and a gait change as speed increases (Scholey, 1983; Rayner, 1991; Tobalske and Dial, 1996). Providing further evidence that the zebra finch is not constrained by the contractile properties of the pectoralis, the duration of electromyographic bursts in the pectoralis varies more between take-off or landing and level flight in the zebra finch than in several species of hummingbird (Trochilidae; Hagiwara et al., 1968).

All existing mathematical models indicate that continuous flapping is expected to require less average mechanical power output than flap-bounding at slow speeds ( $<4\text{ m s}^{-1}$ ), regardless of body lift or lift from the wings during 'pull-out' phases. At slow flight speeds, why did the zebra finch use intermittent bounds to vary power output rather than flap continuously with a lower level of within-wingbeat power? The above analysis suggests that wing morphology, including aspect ratio, was functioning as a constraint, forcing the zebra finch to use intermittent bounds at slow speeds as predicted by one part of the fixed-gear hypothesis.

One functional explanation for this constraint may involve control and maneuverability during slow flight. At a given slow flight speed (e.g.  $2\text{ m s}^{-1}$ ), wing-reversal upstrokes and wingtip-reversal upstrokes may offer more opportunity for fine-scale adjustments in within-wingbeat aerodynamics. The zebra finch is only likely to have the duration of the downstroke, approximately 60% of a wingbeat cycle (Table 2), in which to vary lift production and control body position, because the upstroke is not expected to have any

significant aerodynamic effect in a vortex-ring gait with a feathered upstroke (Rayner, 1991). Brief, intermittent bounds would offer an effective, albeit crude, adjustment in altitude or speed for a species that perhaps seldom engages in steady, slow flight or hovering under natural conditions. In contrast, hummingbirds can vary lift production during their entire wingbeat cycle because they produce lift during both the downstroke and upstroke (Greenewalt, 1960); this would give a hummingbird up to 100% of a wingbeat cycle in which to control its body position. The aerodynamic function of a wingtip-reversal upstroke in a bird such as the budgerigar probably permits some control and maneuvering during the upstroke. Although vortex-visualization studies suggest that the upstroke does not produce lift (Rayner, 1991), kinematic studies (Brown, 1963; Warrick and Dial, 1998) and measurements of strain on feather shafts (Corning and Biewener, 1998) indicate that portions of the wingtip-reversal upstroke in the rock dove (*Columba livia*; pigeon) generate significant profile drag on the wing. Rock doves use their tip-reversal upstroke to help control turns in slow flight (Warrick and Dial, 1998), so it is feasible that a tip-reversal upstroke would help a slow-flying budgerigar control its altitude and speed.

Using a mathematical model, it is predicted that birds with relatively long wings or wings of high aspect ratio should change from a vortex-ring to a continuous-vortex gait as speed increases because a lifting upstroke is aerodynamically inefficient at slow speeds (Rayner, 1993). Although this prediction does not specifically address why a species with a relatively rounded wing or a wing of low aspect ratio should be constrained to use a feathered upstroke instead of a wingtip-reversal upstroke in slow flight, similar reasoning may apply. It is possible that the use of a wingtip-reversal upstroke would have an unduly adverse effect on net weight support and positive thrust per wingbeat in the zebra finch. Unsteady aerodynamic effects probably dominate flapping flight at slow speeds (Spedding, 1993; Vogel, 1994), and current information about these effects in birds is too limited to make quantitative predictions about aerodynamic efficiency. In addition to possible aerodynamic explanations, other factors that might prevent the zebra finch from using a wingtip-reversal upstroke could include neuromuscular control and the anatomy of the skeletal or muscular elements in the wing. Exploring these potential explanations may be worthwhile for future research into gait selection in flying birds.

We assumed in our analysis that the angular velocity of the wing was directly proportional to the contractile velocity in the pectoralis muscle. This assumption appears to be reasonable because recent studies using sonomicrometry measurements have validated estimates of muscle strain and strain rate inferred from wing kinematics (Biewener et al., 1998; Dial et al., 1998). Some differences could nonetheless exist between the timing of wing motion at the flexible wing tip and the contractile activity in the pectoralis (Biewener et al., 1998), so it would be worthwhile to employ sonomicrometry techniques to confirm our present analysis. Ideally, these data could be

coupled with direct measurements of force production to estimate *in vivo* mechanical power output (Dial et al., 1997, 1998; Biewener et al., 1998). Kinematic estimates will probably remain the reference representing normal flap-bounding behavior because surgical implantation of electrodes and transducers, as well as the weight and drag of recording cables, will probably affect intermittent flight performance in small birds such as the zebra finch (Tobalske, 1995).

To provide further insight into the biological significance of the variation in angular velocity of the wing exhibited by the zebra finch (Table 2; Fig. 4), a comparative study using *in vitro* measures of power output and efficiency as a function of strain rate in the pectoralis would be useful (e.g. Barclay, 1996; Askew and Marsh, 1998). This would permit a direct measure of a range of contractile velocities that a muscle may exhibit without a significant drop in power output or efficiency.

#### Body-lift hypothesis

The kinematics of bounds in the zebra finch revealed that Rayner's (1985) model was more accurate with regard to assumptions on flight performance than the models of DeJong (1983) and Ward-Smith (1984a). The zebra finch did not exhibit pull-out phases *sensu* DeJong (1983) during which the wings should be held extended and motionless for a brief period at the end of a bound. At the ends of bounds, the wings were simultaneously elevated and extended (Fig. 6). Ward-Smith's (1984a) model does not include parasite drag during bounds, yet our measurements of body drag indicated that this was a significant component of bounds at flight speeds from 4 to 14 m s<sup>-1</sup> (Fig. 9B). In addition to parasite drag on the body, our measurement of body drag includes profile drag on the folded wing and, potentially, induced drag if body lift involves vortex production. Parasite drag is probably the major component, however, and should not be neglected in models of flap-bounding. Rayner's (1985) model incorporates this source of drag, and potential effects of body lift, so our subsequent discussion will be based largely on this model. Other existing models of flap-bounding are, for practical purposes, identical to Rayner's (1985) analysis (Lighthill, 1977; Alexander, 1982; Azuma, 1992).

The aerodynamic function of bounds in zebra finch changed according to flight speed (Fig. 9) in agreement with predictions of how body lift should be employed according to flight strategy. Body lift is expected to reduce losses in altitude and to increase range during bounds (Csicsáky, 1977a,b). To maximize range, a flap-bounding bird should, therefore, generate body lift during bounds; to maximize speed, the same bird should seek to reduce drag at the expense of lift production. Levels of both lift and drag increased as speed increased from 4 to 10 m s<sup>-1</sup>, but during flight at 12 and 14 m s<sup>-1</sup> parasite drag should have more significance than at other speeds (Pennycuick, 1975; Rayner, 1979), and the zebra finch reduced both body lift and drag below the maximum levels exhibited at 10 m s<sup>-1</sup> (Fig. 9). Further evidence of the change in the aerodynamic function of bounds is provided by the lift:drag ratio, which was highest during flight at 4 m s<sup>-1</sup>,

when range maximization should be a significant issue (Fig. 9C).

The levels of body lift we observed *in vivo* in the zebra finch (Fig. 9) were similar to the values Csicsáky (1977a,b) obtained from plaster-cast models of the zebra finch torso, but our data indicate that a living zebra finch is capable of achieving higher lift:drag ratios at comparable speeds. Specifically, with a wind speed of 4.5 m s<sup>-1</sup> and at a body angle of 20°, Csicsáky's plaster-cast models generated 0.0159 N of body lift and achieved a maximum lift:drag ratio of 1.18. Body lift in the live birds in our study was 0.0119 N at 4 m s<sup>-1</sup> and 0.0156 N at 6 m s<sup>-1</sup>; lift:drag ratios were 3.10 and 1.78, respectively, at these two speeds (Fig. 9C). Our measure of body angle relative to horizontal (Figs 7, 8) is not equivalent to Csicsáky's (1977a,b) measure relative to incident air, because the living birds travelled through an arc so that the incident angle was less than the angle relative to horizontal while the bird was gaining altitude and greater than the angle relative to horizontal when the bird was losing altitude (Figs 7, 8; see Csicsáky, 1977a,b; Scholey, 1983).

In the absence of any body lift, flap-bounding is predicted to have an aerodynamic advantage at speeds greater than approximately 1.2V<sub>mr</sub> (Rayner, 1985). This saving is due to folding the wings, which effectively eliminates profile drag during bounds. According to Rayner (1985), V<sub>mr</sub> for the zebra finch is 5.9 m s<sup>-1</sup>, so the critical speed for an aerodynamic advantage is approximately 7.1 m s<sup>-1</sup>. The zebra finches readily flew at twice this speed in the wind tunnel (Figs 4, 5), so even without body lift, they probably obtained an aerodynamic advantage over continuous flapping. The body lift generated during bounds at flight speeds from 8 to 14 m s<sup>-1</sup> (Fig. 9) probably functioned to increase this advantage. This may explain why the percentage of time spent flapping decreased with increasing speed rather than varying with speed according to a U-shaped curve (Fig. 5A). Not surprisingly, the birds appeared to be most comfortable in flight at the faster flight speeds. They readily flew for longer with less need for encouragement.

We must calculate the minimum required body lift that would make mechanical power output lower during flap-bounding than during continuous flapping to evaluate whether the observed body lift could have offered an aerodynamic advantage to the zebra finches during flight at speeds slower than 1.2V<sub>mr</sub> (i.e. <7.1 m s<sup>-1</sup>). There is a predicted aerodynamic advantage to flap-bounding if:

$$b > 0.5 \left\{ 1 - \left[ 1 + \left( \frac{A_b}{A_w} \right) \right]^{-1} \left( \frac{V}{V_{mr}} \right)^4 \right\}, \quad (4)$$

where  $b$  is the proportion of body weight supported,  $A_b$  is the parasite drag on the body,  $A_w$  is the profile drag on the wings,  $V$  is body velocity and  $V_{mr}$  is the maximum range speed (Rayner, 1985). Values for  $A_b/A_w$  are not known, and this is the critical component of the equation at any given speed because lower values of  $A_b/A_w$  will yield lower estimates for  $b$ . For  $A_b/A_w$ , Rayner (1985) suggested a value of 1, with

possible variation between 0.5 and 2. For the zebra finches in our study, observed  $b=0.1202$  at  $6\text{ m s}^{-1}$ ; this value satisfies equation 4 at a flight speed of  $6.095\text{ m s}^{-1}$  when  $A_b/A_w=0.5$  and at a speed of  $6.550\text{ m s}^{-1}$  when  $A_b/A_w=1.0$ . Stated another way, at  $5.9\text{ m s}^{-1}$ ,  $A_b/A_w$  at the observed  $b$  would have had to increase by 0.046 (or 4.6% of body weight) to satisfy equation 4. On the basis of these calculations, observed values of body lift appeared to be close enough to required values to conclude that flap-bounding was an aerodynamically attractive flight strategy at our measured speed of  $6\text{ m s}^{-1}$ , and observed body lift approached being sufficient to make flap-bounding potentially more attractive than continuous flapping at  $V_{mr}$  ( $5.9\text{ m s}^{-1}$ ). The same, however, cannot be said for slower speeds. At  $4\text{ m s}^{-1}$ , observed  $b$  was 0.091 (Fig. 9), and minimum required  $b$  is estimated to be 0.430 if  $A_b/A_w=0.5$  and 0.448 if  $A_b/A_w=1.0$ . No advantage was likely to be available at  $2\text{ m s}^{-1}$ , because body lift was 0 N (Fig. 9), and body lift was logically 0 N during hovering. Thus, the body-lift hypothesis appeared to account for the use of flap-bounding flight at moderate and fast flight speeds ( $6\text{--}14\text{ m s}^{-1}$ ), but was inadequate to explain the use of bounds during slower-speed flight ( $0\text{--}4\text{ m s}^{-1}$ ).

Slight spreading of the wings during the upstroke at intermediate flight speeds ( $6\text{--}10\text{ m s}^{-1}$ ; Table 2; Fig. 3A) could function to decrease levels of body lift required to satisfy equation 4; this would increase the savings offered by flap-bounding at these speeds. The observed differences in upstroke span represented variation within what we interpreted to be a vortex-ring gait (Rayner, 1991). Normally, it is not expected that the wings should produce lift during the upstroke in the vortex-ring gait with a feathered upstroke, but it is logical to expect that, if the body can produce lift without wing spreading (Figs 3B, 9), slight wing spreading during the upstroke (Fig. 3A) should have some aerodynamic effect at intermediate and fast flight speeds.

#### *Effects of the wind tunnel*

Bird flight performance may be affected by the artificial nature of flight in a wind tunnel (Rayner, 1994). We estimate that wind-tunnel effects were minimal in the present study because the birds appeared to be well acclimated to the experimental conditions and because of the large size of the flight chamber compared with the size of the zebra finch. Flight speeds and mechanical power requirements are expected to decrease in the closed section of a wind tunnel in comparison with free flight in the absence of ground effects, and the decreases are expected to be greatest at slower speeds (Rayner, 1994); this should be taken into account when interpreting our results.

To calculate the appropriate aerodynamic corrections, one must take into account the position of the bird within the flight chamber. In a cross-sectional view, the birds generally flew centered horizontally, between the midline and the upper quarter vertically ( $h/H$  values of  $0\text{--}0.25$ , where  $h$  is the altitude of the body above the midline of the chamber and  $H$  is the vertical height of the chamber; Rayner 1994). The tabular data

presented in Rayner (1994) for such a body position, and a diameter of flight chamber to wing span ratio of 3, indicate that the minimum power speed ( $V_{mp}$ ) and maximum range speed ( $V_{mr}$ ) were reduced by 2.5 and 2.0%, respectively, and the mechanical power at these speeds was reduced by 5.7 and 3.7%, respectively, in comparison with conditions in free flight. These magnitudes represent slight overestimates for the zebra finch, because the diameter of the flight chamber of our tunnel was 4.5 times larger than the wing span of the zebra finch.

It will always be true that a bird flying in a wind tunnel in a laboratory is experiencing unusual conditions relative to free flight outdoors. Field work is needed to account fully for this inherent limitation in the present study. Tobalske et al. (1997) provide an example of this combined approach to the study of bird flight. Unfortunately, it is nearly impossible to observe the same bird flying over a wide range of flight speeds in the field.

#### *Comparative aspects of intermittent flight*

Certain aspects of wing and body motion during flap-bounding in the zebra finch were similar to patterns observed during flap-bounding in other species. For example, body angle in the budgerigar decreases during bounds as in the zebra finch (Fig. 8). A general pattern among birds that flap-bound seems to be that the wings are drawn into a bound posture during the upstroke and that wing flapping resumes after the bound using the upstroke (e.g. Tobalske, 1996; Figs 6, 8). Similarly, other species exhibit variation in wingtip elevation within flapping phases (Fig. 6). Wingbeats with increased frequency and elevation generally correspond to forward and upward acceleration during the flapping phase (Tobalske, 1995; Tobalske and Dial, 1996; Tobalske et al., 1997).

Because they used flap-bounding at all flight speeds, the zebra finches exhibited a different style of flight compared with birds such as swallows (Hirundinidae), budgerigars, European starlings *Sturnus vulgaris*, Lewis's woodpeckers (*Melanerpes lewis*) and black-billed magpies that facultatively shift from flap-gliding at slow or intermediate speeds to flap-bounding at fast speeds (Tobalske and Dial, 1994, 1996; Tobalske, 1995, 1996; Warrick, 1998; D. Warrick, personal communication). The species that shift intermittent flight styles vary in body mass from 13 to 159 g and differ with respect to aspect ratio and distal wing shape. Some of the larger species may be unable to bound at all speeds because of the adverse scaling of available power or lift per unit power output (Pennycuik, 1975; DeJong, 1983; Marden, 1994), so they might, therefore, resort to gliding instead of bounding (Rayner, 1985; Tobalske and Dial, 1996). Swallows (13–19 g) and budgerigars have wings of higher aspect ratio than those of the zebra finch (Warrick, 1998; Table 1), which may indicate that their wings offer higher lift:drag ratios (Vogel, 1994) so that flap-gliding could offer more of a saving in average mechanical power than flap-bounding at intermediate flight speeds. These ideas should be tested to elucidate both functional significance and phylogenetic trends.

*Predictions for flight speeds in nature*

From our comparative analyses, we observed that wings of low aspect ratio (rather than pectoralis composition) may constrain the zebra finch to use intermittent bounds rather than continuous flapping during slow flight, as suggested by one part of the fixed-gear hypothesis (Rayner, 1985; Azuma, 1992). Because flap-bounding is not expected to be efficient relative to continuous flapping at slow speeds (Lighthill, 1977; Rayner, 1977, 1985; Alexander, 1982; DeJong, 1983; Ward-Smith, 1984a,b; Azuma, 1992), we suggested that the zebra finch may use bounds as a relatively crude control mechanism for body position in slow flight. This implies that the zebra finch is not well designed for hovering or slow flight, so we predict that zebra finches, and similarly shaped flap-bounding birds, seldom engage in steady hovering or slow flight in the wild. Greenewalt (1960) observed that particularly small birds that use feathered upstrokes may accelerate rapidly to faster speeds after take-off. This is consistent with DeJong's (1983) observation that acceleration ability scales negatively with increasing body mass in flap-bounding birds.

The percentage of time spent flapping decreased with airspeed (Fig. 5A), and this provides one estimate of the shape of the mechanical power curve for zebra finch flight (mechanical power is zero during bounds). To provide a better approximation of the shape of the curve for mechanical power, changes in angular velocity of the wing (Fig. 4C) should be taken into account. The values for this variable were smallest at intermediate speeds, which suggests that the mechanical power curve was more upwardly concave than the curve for percentage of time spent flapping would indicate. Nonetheless, the curve for the percentage of time spent flapping (Fig. 4A) is the best approximation available in the absence of *in vivo* measures of power output (e.g. Dial et al., 1997; Biewener et al., 1998).

From the curve for percentage of time spent flapping (Fig. 5A), we may infer that the cost of transport, defined as mechanical work per unit distance, should approach a minimum as speed increases in a flap-bounding zebra finch. If reducing the cost of transport was a goal, as might be expected during migration or long-distance flight, we predict that a flap-bounding zebra finch should fly quite fast (i.e. 12–14 m s<sup>-1</sup>); adjusting this rough estimate of  $V_{mr}$  according to variation in the angular velocity of the wing may mean that  $V_{mr}$  for the flap-bounding zebra finch is nearer 10 or 12 m s<sup>-1</sup>. It will be interesting to see how these predictions of  $V_{mr}$  compare with actual speeds used by flap-bounding birds engaged in long-distance flight the wild.

**List of symbols**

$A_b$	parasite drag on the body
$A_w$	profile drag on the wings
$B_a$	wing span at the start of downstroke
$B_b$	wing span at the end of downstroke
$b$	proportion of body weight supported during a bound

$H$	vertical height of flight chamber
$h$	altitude of the body above the midline of the flight chamber
$S_d$	disk area of the wings
$V$	body velocity
$V_f$	flapping velocity
$V_i$	vertical component of induced velocity
$V_{mr}$	maximum range speed
$V_{mp}$	minimum power speed
$W$	body weight
$WA$	wingbeat amplitude
$WE_a$	wingtip elevation at the start of downstroke
$WE_b$	wingtip elevation at the end of downstroke
$X$	distance between shoulder joints
$\alpha$	angle of incidence of the wing
$\beta$	body angle relative to horizontal.
$\delta_b$	stroke-plane angle relative to the body
$\delta_h$	stroke-plane angle relative to horizontal.
$\phi$	pronation angle of the wing
$\rho$	air density

We thank Kathleen Ores for training the birds and assisting with filming and Doug Warrick for providing helpful discussion during all phases of this project. Matt Bundle provided video recordings of budgerigar flight, for which we are grateful. B.W.T. also wishes to thank Claudine Tobalske for encouragement and Andrew Biewener for financial support and working space during the analysis of the data and preparation of the manuscript. This study was supported in part by National Science Foundation Grant IBN-9507503 to K.P.D.

**References**

- Aldridge, H. D. J. N.** (1986). Kinematics and aerodynamics of the greater horseshoe bat, *Rhinolophus ferrumequinum*, in horizontal flight at various flight speeds. *J. Exp. Biol.* **126**, 479–497.
- Alexander, R. McN.** (1982). *Optima for Animals*. London: Arnold.
- Askew, G. N. and Marsh, R. L.** (1998). Optimal shortening velocity ( $V/V_{max}$ ) of skeletal muscle during cyclical contractions: length–force effects and velocity-dependent activation and deactivation. *J. Exp. Biol.* **201**, 1527–1540.
- Azuma, A.** (1992). *The Biokinetics of Flying and Swimming*. New York: Springer-Verlag.
- Barclay, C. J.** (1996). Mechanical efficiency and fatigue of fast and slow muscles of the mouse. *J. Physiol., Lond.* **497**, 781–794.
- Biewener, A. A., Corning, W. R. and Tobalske, B. W.** (1998). *In vivo* pectoralis muscle force–length behavior during level flight in pigeons (*Columba livia*). *J. Exp. Biol.* **201**, 3293–3307.
- Bilo, D.** (1971). Flugbiophysik von Kleinvögeln. I. Kinematik und Aerodynamik des Flügelabschlages beim Haussperling (*Passer domesticus*). *Z. Vergl. Physiol.* **71**, 382–454.
- Bilo, D.** (1972). Flugbiophysik von Kleinvögeln. II. Kinematik und Aerodynamik des Flügelauflages beim Haussperling (*Passer domesticus*). *Z. Vergl. Physiol.* **76**, 426–437.
- Brown, R. H. J.** (1963). The flight of birds. *Biol. Rev.* **38**, 460–489.
- Corning, W. R. and Biewener, A. A.** (1998). *In vivo* strains in pigeon

- flight feather shafts: implications for structural design. *J. Exp. Biol.* **201**, 3057–3065.
- Csicsáky, M. J.** (1977a). Aerodynamische und Ballistische Untersuchungen an Kleinvögeln. PhD thesis, University of Hamburg.
- Csicsáky, M. J.** (1977b). Body-gliding in the zebra finch. *Fortschr. Zool.* **24**, 275–286.
- Danielson, R.** (1988). Parametre for fritflyvende småfugles flugt. *Dan. Orn. Foren. Tidsskr.* **82**, 59–60.
- Dejong, M. J.** (1983). Bounding flight in birds. PhD thesis, University of Wisconsin, Madison.
- Dial, K. P.** (1992). Avian forelimb muscles and nonsteady flight: can birds fly without using the muscles in their wings? *Auk* **109**, 874–885.
- Dial, K. P., Biewener, A. A., Tobalske, B. W. and Warrick, D. R.** (1997). Mechanical power output of bird flight. *Nature* **390**, 67–70.
- Dial, K. P., Warrick, D. R., Tobalske, B. W. and Biewener, A. A.** (1998). Power output of magpies: estimates of humeral excursion via pectoral sonomicrometry and wing kinematics. *Am. Zool.* **38**, 152A.
- Dunning, J. B., Jr** (1993). *CRC Handbook of Avian Body Masses*. Boca Raton, FL: CRC Press.
- Goldspink, G.** (1977). Mechanics and energetics of muscle in animals of different sizes, with particular reference to the muscle fibre composition of vertebrate muscle. In *Scale Effects in Animal Locomotion* (ed. T. J. Pedley), pp. 37–55. New York: Academic Press.
- Goldspink, G.** (1981). The use of muscles during flying, swimming and running from the point of view of energy saving. *Symp. Zool. Soc., Lond.* **48**, 219–238.
- Greenewalt, C. H.** (1960). *Hummingbirds*. New York: Doubleday.
- Hagiwara, S., Chichibu, S. and Simpson, N.** (1968). Neuromuscular mechanisms of wing beat in hummingbirds. *Z. Vergl. Physiol.* **60**, 209–218.
- Hill, A. V.** (1950). The dimensions of animals and their muscular dynamics. *Sci. Prog.* **38**, 209–230.
- Kokshaysky, N. V.** (1979). Tracing the wake of a flying bird. *Nature* **279**, 146–148.
- Lide, D. R.** (1998). *CRC Handbook of Chemistry and Physics*, 79th edition 1998–1999. Boca Raton, FL: CRC Press.
- Lighthill, M. J.** (1977). Introduction to the scaling of aerial locomotion. In *Scale Effects in Animal Locomotion* (ed. T. J. Pedley), pp. 365–404. New York: Academic Press.
- Marden, J.** (1994). From damselflies to pterosaurs: how burst and sustainable flight performance scale with size. *Am. J. Physiol.* **266**, R1077–R1084.
- Pennycuik, C. J.** (1975). Mechanics of flight. In *Avian Biology*, vol. 5 (ed. D. S. Farner and J. R. King), pp. 1–75. London: Academic Press.
- Pye, J. D.** (1981). Echolocation for flight guidance and a radar technique applicable for flight analysis. *Symp. Zool. Soc. Lond.* **48**, 199–218.
- Rayner, J. M. V.** (1977). The intermittent flight of birds. In *Scale Effects in Animal Locomotion* (ed. T. J. Pedley), pp. 37–55. New York: Academic Press.
- Rayner, J. M. V.** (1979). A new approach to animal flight mechanics. *J. Exp. Biol.* **80**, 17–54.
- Rayner, J. M. V.** (1985). Bounding and undulating flight in birds. *J. Theor. Biol.* **117**, 47–77.
- Rayner, J. M. V.** (1991). Wake structure and force generation in avian flapping flight. *Acta XX Cong. Int. Orn.* **II**, 702–715.
- Rayner, J. M. V.** (1993). On aerodynamics and the energetics of vertebrate flapping flight. *Cont. Math.* **141**, 351–400.
- Rayner, J. M. V.** (1994). Aerodynamic corrections for the flight of birds and bats in wind tunnels. *J. Zool., Lond.* **234**, 537–563.
- Rosser, B. W. C. and George, J. C.** (1986). The avian pectoralis: histochemical characterization and distribution of muscle fiber types. *Can. J. Zool.* **64**, 1174–1185.
- Rosser, B. W. C., Wick, M., Waldbillig, D. M. and Bandman, E.** (1996). Heterogeneity of myosin heavy-chain expression in fast-twitch fiber types of mature avian pectoralis muscle. *Biochem. Cell Biol.* **74**, 715–728.
- Scholey, K. D.** (1983). Developments in vertebrate flight: climbing and gliding of mammals and reptiles and the flapping flight of birds. PhD thesis, University of Bristol.
- Spedding, G. R.** (1987). The wake of a kestrel (*Falco tinnunculus*) in flapping flight. *J. Exp. Biol.* **127**, 59–78.
- Spedding, G. R.** (1993). On the significance of unsteady effects in the aerodynamic performance of flying animals. *Cont. Math.* **141**, 401–419.
- Thomas, A. L. R.** (1993). On the aerodynamics of birds' tails. *Phil. Trans. R. Soc. Lond. B* **340**, 361–380.
- Tobalske, B. W.** (1995). Neuromuscular control and kinematics of intermittent flight in European starlings (*Sturnus vulgaris*). *J. Exp. Biol.* **198**, 1259–1273.
- Tobalske, B. W.** (1996). Scaling of muscle composition, wing morphology and intermittent flight behavior in woodpeckers. *Auk* **113**, 151–177.
- Tobalske, B. W. and Dial, K. P.** (1994). Neuromuscular control and kinematics of intermittent flight in budgerigars (*Melopsittacus undulatus*). *J. Exp. Biol.* **187**, 1–18.
- Tobalske, B. W. and Dial, K. P.** (1996). Flight kinematics of black-billed magpies and pigeons over a wide range of speeds. *J. Exp. Biol.* **199**, 263–280.
- Tobalske, B. W., Olson, N. E. and Dial, K. P.** (1997). Flight style of the black-billed magpie: variation in wing kinematics, neuromuscular control and muscle composition. *J. Exp. Zool.* **279**, 313–329.
- Vogel, S. V.** (1994). *Life in Moving Fluids: The Physical Biology of Flow*, 2nd edn. Princeton: Princeton University Press.
- Von Ende, C. N.** (1993). Repeated-measures analysis: growth and other time-dependent measures. In *Design and Analysis of Ecological Experiments* (ed. S. M. Scheiner and J. Gurevitch), pp. 113–137. New York: Chapman & Hall.
- Ward-Smith, A. J.** (1984a). Analysis of the aerodynamic performance of birds during bounding flight. *Math. Biosci.* **68**, 137–147.
- Ward-Smith, A. J.** (1984b). Aerodynamic and energetic considerations relating to undulating and bounding flight in birds. *J. Theor. Biol.* **111**, 407–417.
- Warrick, D. R.** (1998). The turning- and linear-maneuvering performance of birds: the cost of efficiency for courasing insectivores. *Can. J. Zool.* **76**, 1063–1079.
- Warrick, D. R. and Dial, K. P.** (1998). Kinematic, aerodynamic and anatomical mechanisms in the slow, maneuvering flight of pigeons. *J. Exp. Biol.* **201**, 655–672.
- Woicke, M. and Gewecke, M.** (1978). Kinematic and aerodynamic parameters in tethered flying siskins (*Carduelis spinus*, Passeres, Aves). *J. Comp. Physiol.* **127**, 123–129.